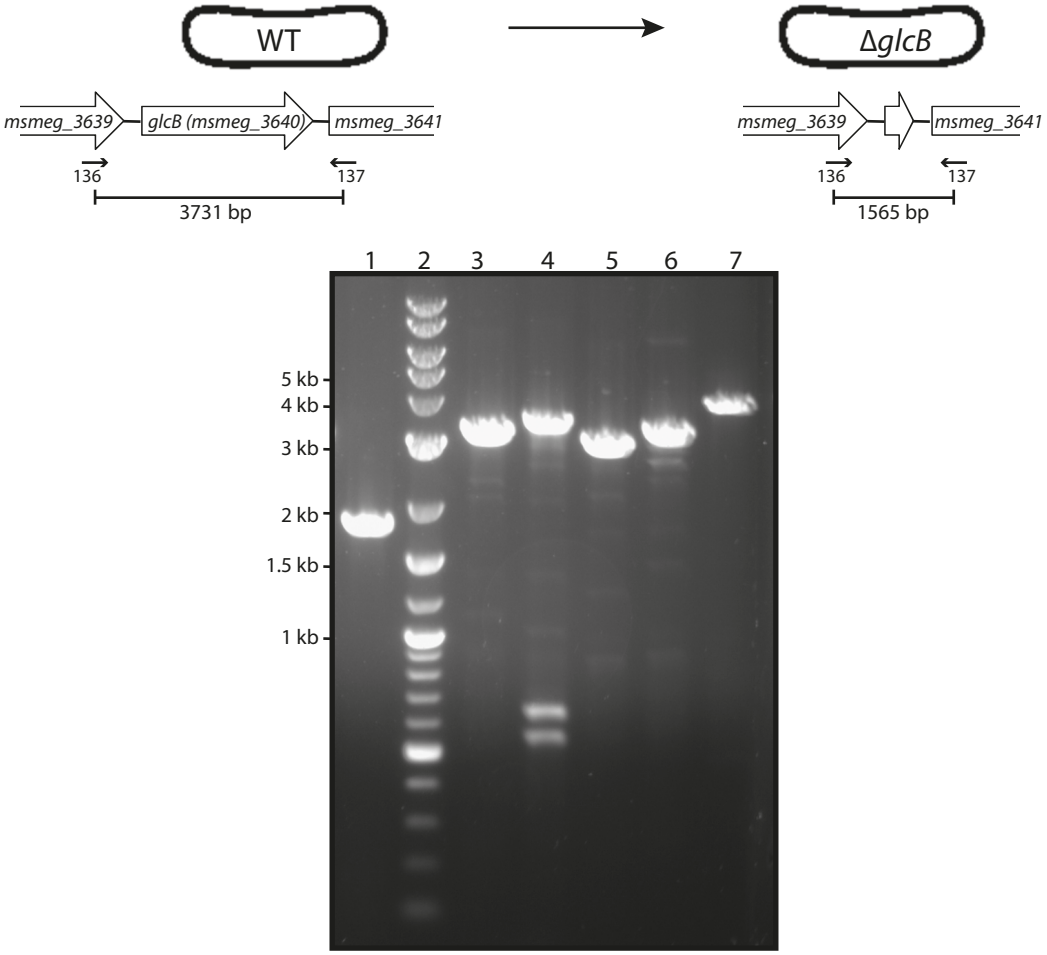

Supplemental Fig. S1. Confirmation of the Δ*glcB* deletion strain.
The Δ*glcB* strain was checked for *glcB* deletion by PCR analysis using oligonucleotides 136 and 137 flanking the *glcB* gene (supplemental Table S1). Lane 1: M. smegmatis Δ*glcB* strain (expected band size: 1,565 bp). Lane 2: Molecular weight markers. Lanes 3-6: DNA fragments of sizes 3,112 bp, 3,375 bp, 2,903 bp, 3,058 bp. Lane 7: *M. smegmatis* wild-type strain (expected band size: 3,731 bp).

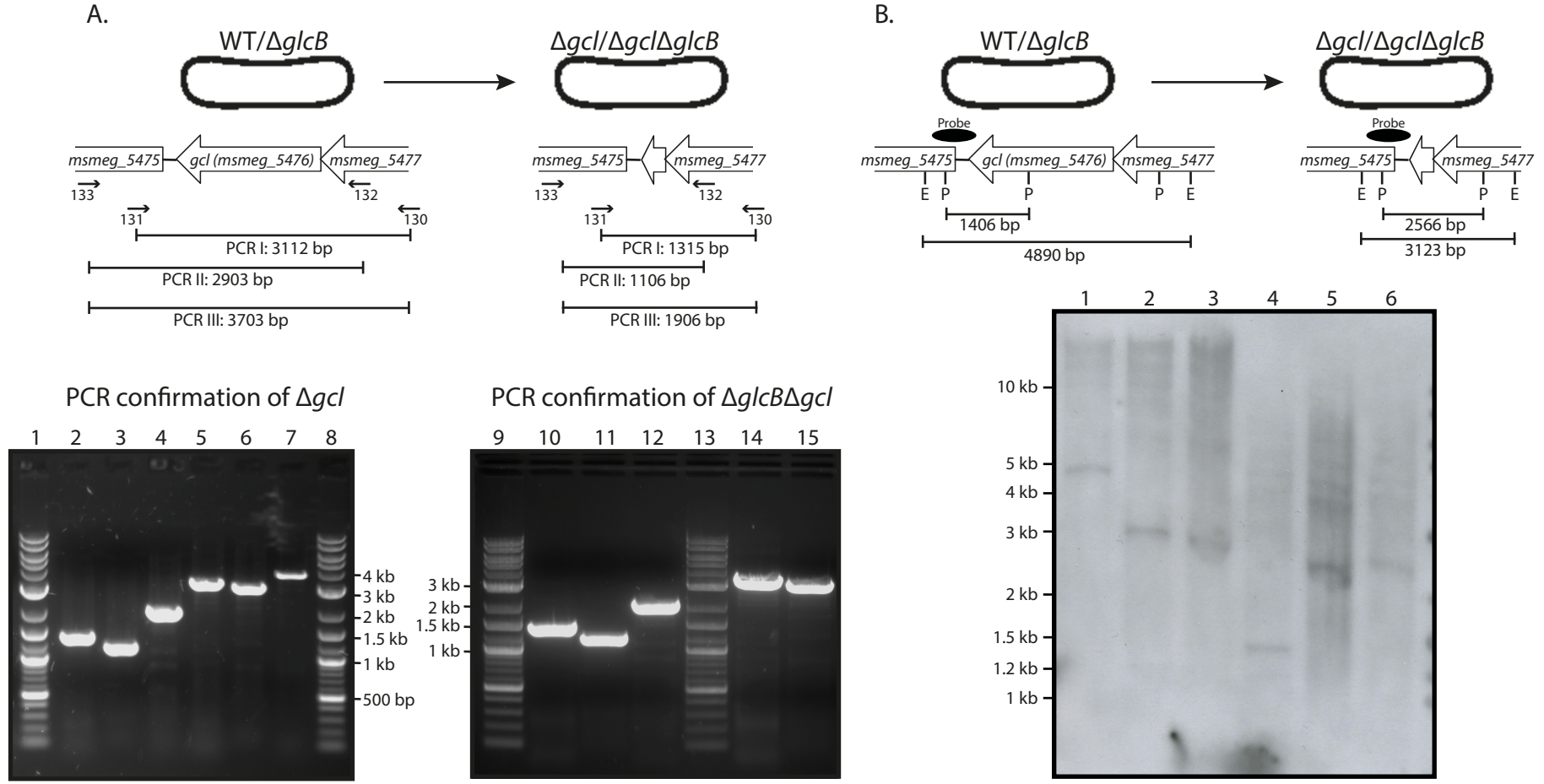

Supplemental Fig. S2. Confirmation of the Δ*gcl* and Δ*glcB*Δ*gcl* deletion strains.

(A) PCR confirmation of Δ*gcl* and Δ*glcB* Δ*gcl* deletion strains. Oligonucleotide sequences are indicated in supplemental Table S1. Lanes 1, 8, 9, 13: Molecular weight marker. Lanes 2, 3, 4: *M. smegmatis* Δ*gcl* strain PCR reactions I, II, III. Lanes 5, 6, 7: *M. smegmatis* wild-type strain PCR reactions I, II, III. Lanes 10, 11, 12: *M. smegmatis* Δ*glcB* Δ*gcl* strains PCR reactions I, II, III. Lanes 14, 15: *M. smegmatis* wild-type strain PCR reactions I, II.

(B) Southern blot confirmation of *gcl* deletion in Δ*gcl* and Δ*glcB* Δ*gcl* strains. Restriction endonuclease sites *PstI* (P) and *EcoRI* (E) are marked with the corresponding sizes for wild-type and gene deletion strains. Probe is indicated by the black oval. Lanes 1, 4: wild-type genomic DNA cut with *EcoRI* (lane 1) or *PstI* (lane 4). Lanes 2, 5: Δ*gcl* genomic DNA cut with *EcoRI* (lane 2) or *PstI* (lane 5). Lanes 3, 6: Δ*glcB* Δ*gcl* genomic DNA cut with *EcoRI* (lane 3) or *PstI* (lane 6).

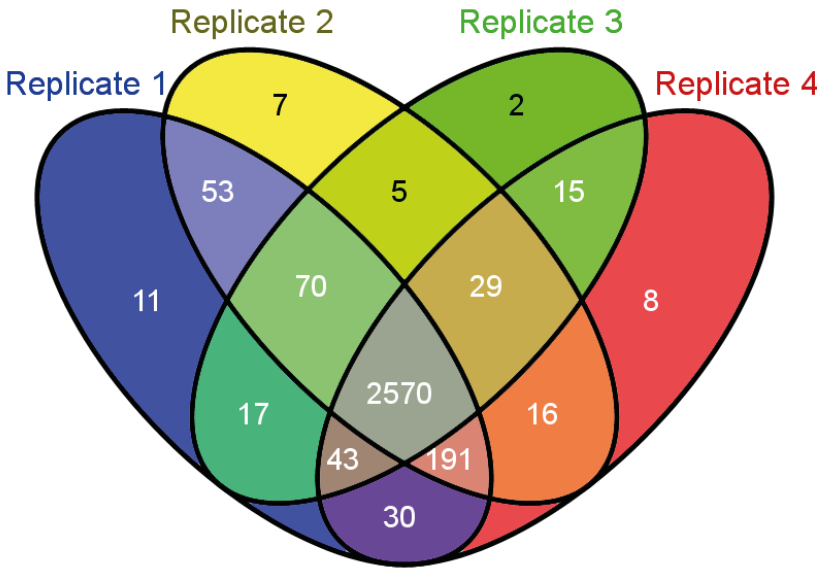

Supplemental Fig. S3. Venn diagram showing proteins identified in four experimental repeats.
The Venn diagram was drawn with the help of VENNY tool (http://bioinfogp.cnb.csic.es/tools/venny/index.html). A total of 2,570 proteins were identified in all four experimental repeats and an additional 333 (=70+191+29+43) were identified in at least three out of the four repeats.

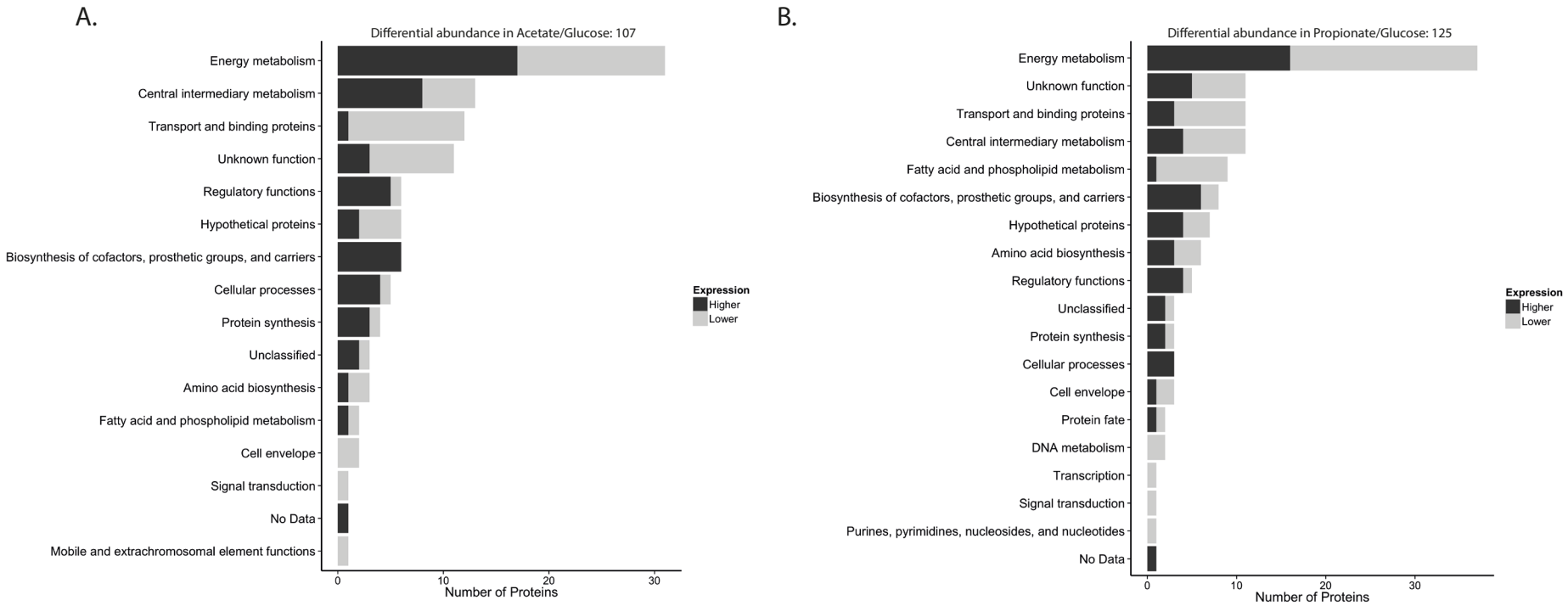

Supplemental Fig. S4. Functional classification of identified and differentially abundant *M. smegmatis* proteins.
Proteins were classified according to their JCVI annotations (http://cmr.jcvi.org). (A) Proteins that were differentially abundant in acetate-grown versus glucose-grown cells. (B) Proteins that were differentially abundant in propionate-grown versus glucose-grown cells. Black and grey shading indicates proteins showing higher and lower abundance, respectively.

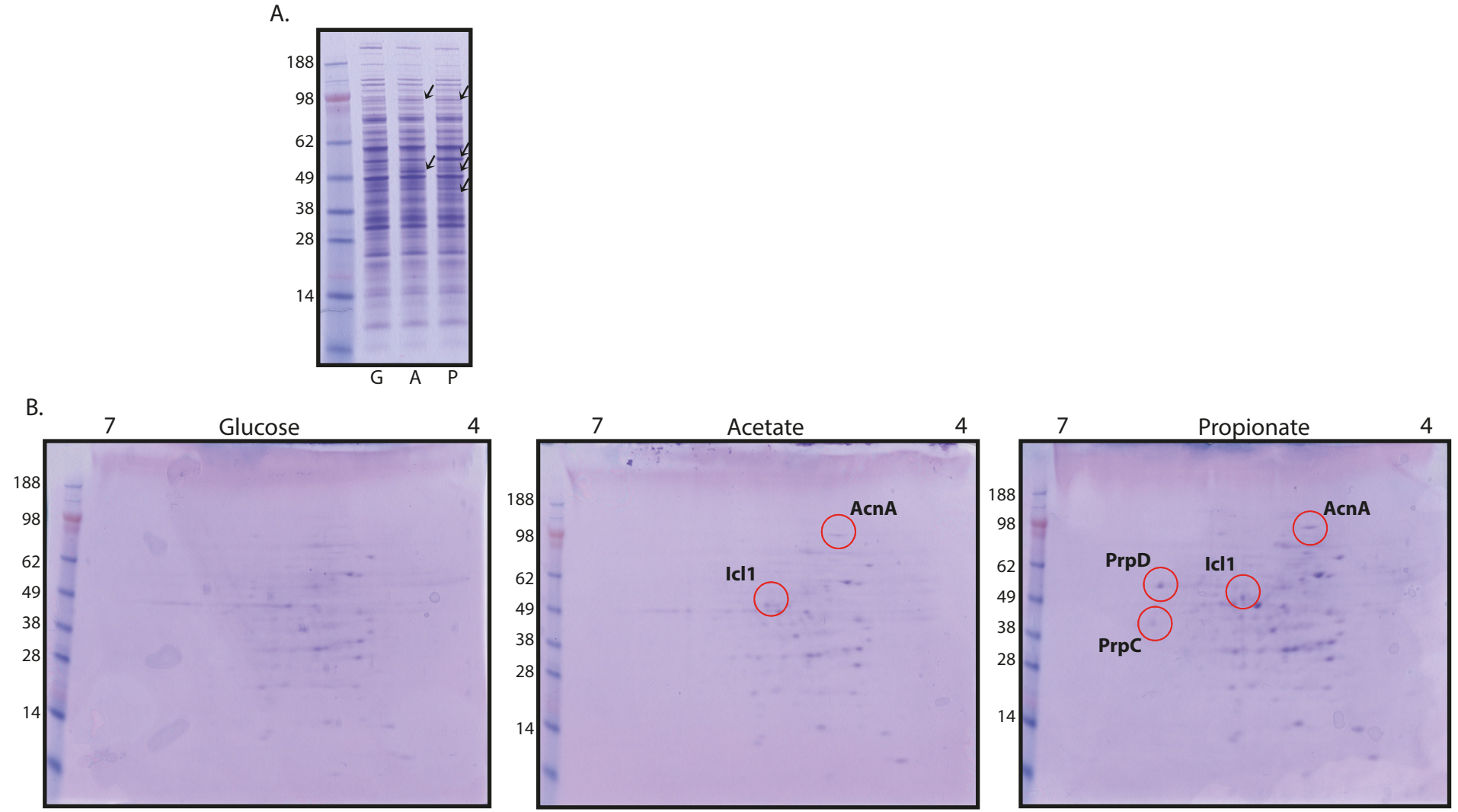

Supplemental Fig. S5. Confirmation of representative proteins showing increased abundance during growth on acetate or propionate as the sole carbon source.

Size fractionation was performed by SDS-PAGE analysis on 4-12% NuPAGE gels using MES running buffer (Invitrogen) accordingly to manufacturer's instructions. The gels were stained with Coomassie Brilliant Blue R-250.

(A) *M. smegmatis* whole-cell lysates were prepared from cells grown on glucose (G), acetate (A), or propionate (P) as the sole carbon source and 5 µg of each lysate was separated on a SDS-PAGE gel. Proteins showing differential abundance are indicated by an arrow.

(B) Low-resolution 2D-PAGE analysis of whole-cell lysates (100 µg each) from cells grown on glucose, acetate, or propionate as the carbon source. The lysates were separated in the first dimension on a pH 4-7 gradient and then in the second dimension on a denaturing SDS-PAGE gel. Protein spots showing differential abundance are marked and the mass spectrometric identification results are indicated.

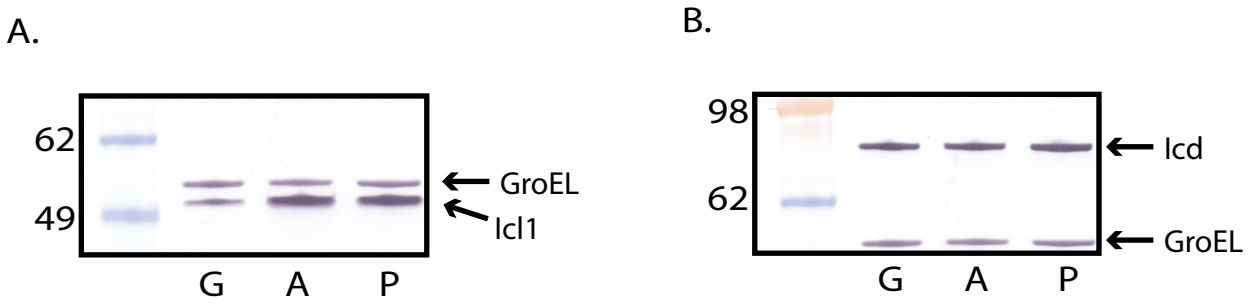

Supplemental Fig. S6. Immunoblot validation of Icl1 and Icd proteins in whole-cell lysates.
M. smegmatis whole-cell lysates were prepared from cells grown on glucose (G), acetate (A), or propionate (P) as the sole carbon source. 5 µg of each lysate was separated on a SDS-PAGE gel, transferred to a nitrocellulose membrane, and probed with GroEL+FLAG antibody to detect FLAG-tagged Icl1 (A) and GroEL+HA antibody to detect HA-tagged Icd (B). Size fractionation was performed by SDS-PAGE analysis on 4-12% NuPAGE gels using MES running buffer accordingly to the manufacturer's instructions (Invitrogen). Proteins were transferred onto nitrocellulose membranes using the iBlot system (Invitrogen). Membranes were blocked with 5% milk and then probed with specific primary antibodies (FLAG tag, Clone M2, Sigma; HA tag, Clone 16B12, Covance; GroEL2, IT-70). All antibodies were used at a dilution of 1:1,000 except for anti-GroEL2 (1:5,000). The secondary antibody was HRP-conjugated anti-mouse antibody (DakoCytomation). The target band was colorimetrically detected using the Opti-4CN kit (Bio-Rad). The IT-70 antibody was obtained through the NIH Biodefense and Emerging Infections Research Resources Repository, NIAID, NIH: monoclonal anti-Mycobacterium tuberculosis GroEL2 (Gene Rv0440), Clone IT-70 (DCA4), NR-13657.

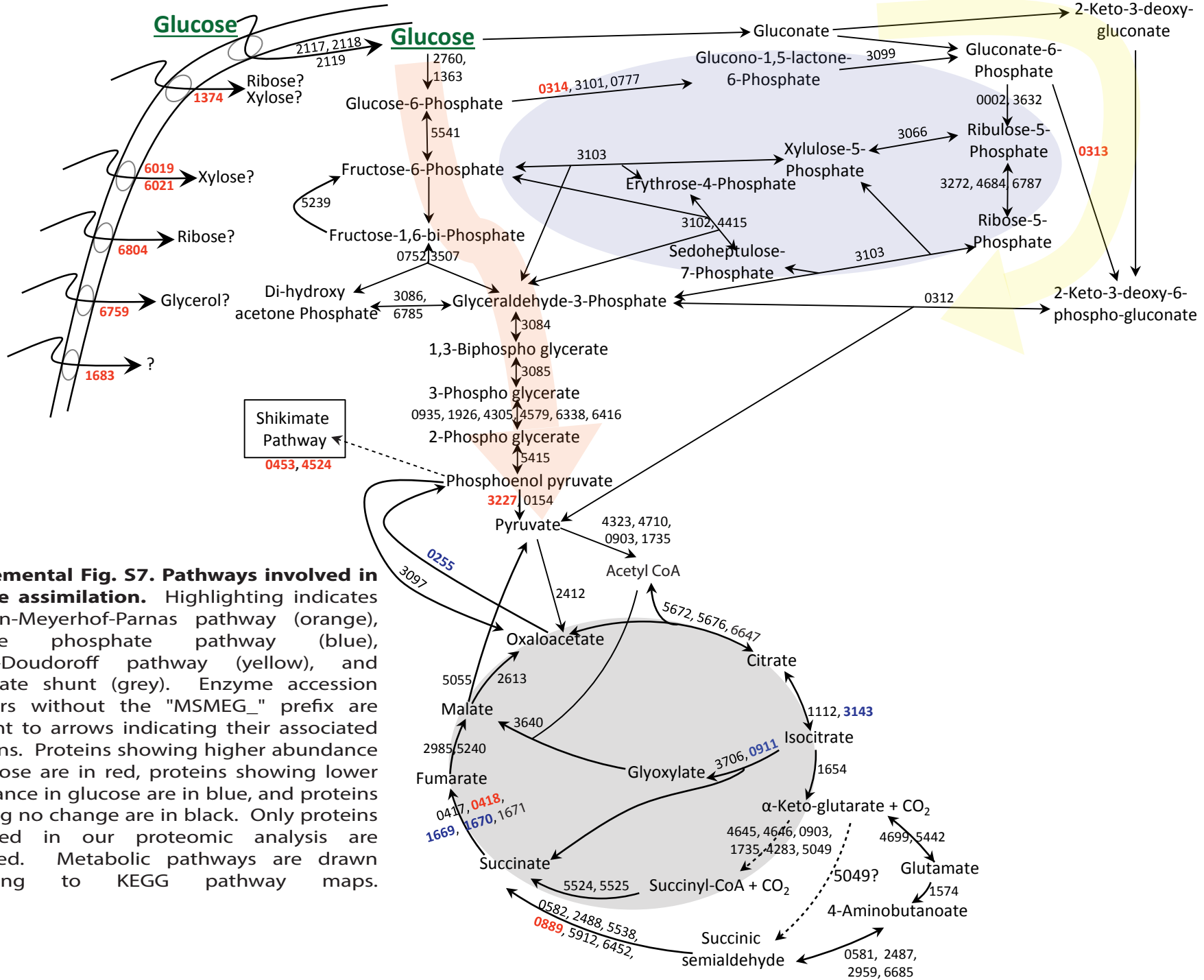

Supplemental Fig. S7. Pathways involved in glucose assimilation. Highlighting indicates Embden-Meyerhof-Parnas pathway (orange), pentose phosphate pathway (blue), Entner-Doudoroff pathway (yellow), and glyoxylate shunt (grey). Enzyme accession numbers without the "MSMEG_" prefix are adjacent to arrows indicating their associated reactions. Proteins showing higher abundance in glucose are in red, proteins showing lower abundance in glucose are in blue, and proteins showing no change are in black. Only proteins identified in our proteomic analysis are indicated. Metabolic pathways are drawn according to KEGG pathway maps.

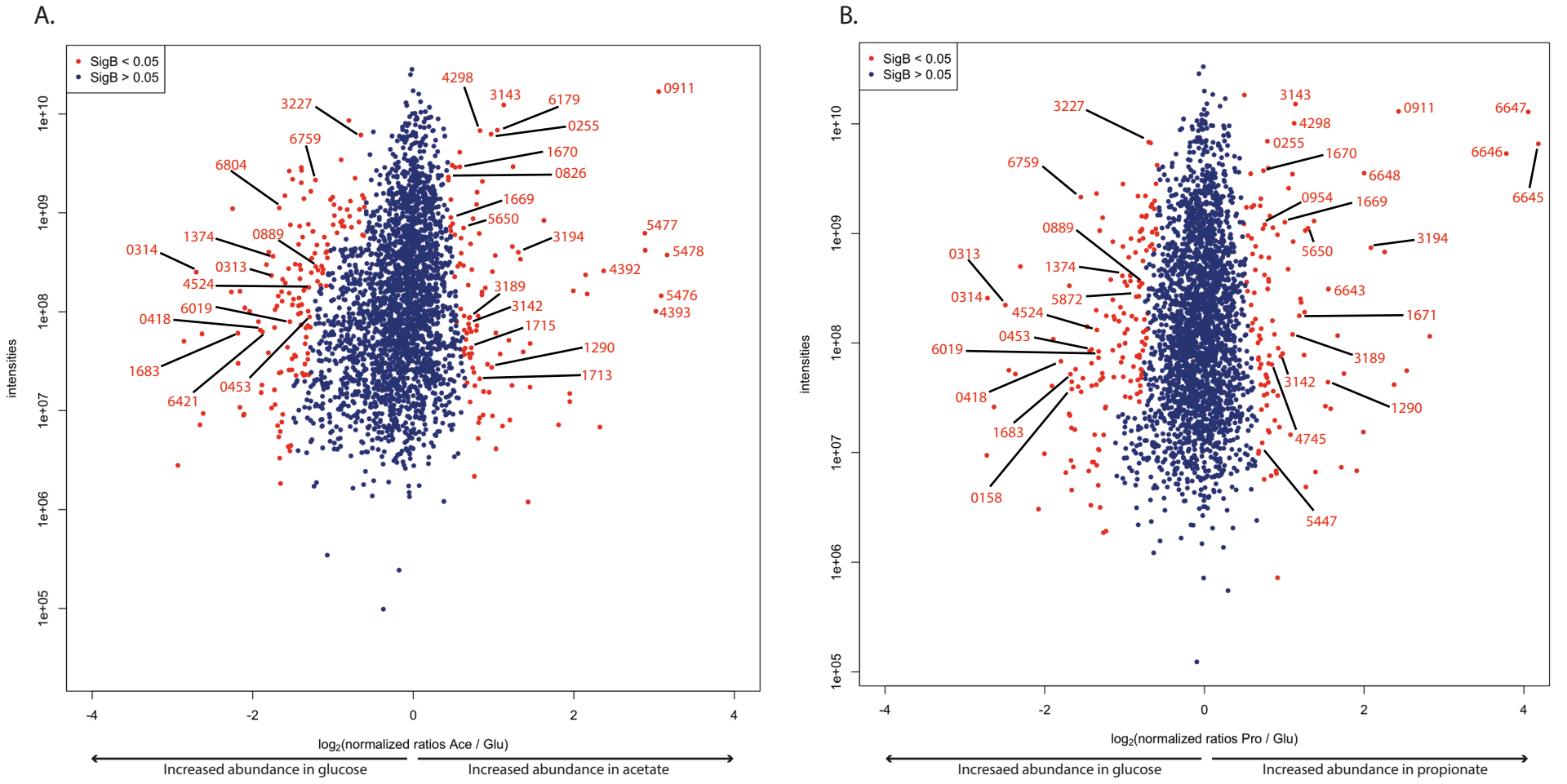

Supplemental Fig. S8. Scatter plot depicting differential abundance of proteins in cells grown on glucose, acetate, or propionate as the sole carbon source.

Each dot represents the summed peptide intensities for a particular protein. Protein abundances are indicated on the y-axes and their relative increase or decrease in acetate/glucose (A) and propionate/glucose (B) ratios are indicated on the x-axes. Proteins in red have SignB values < 0.05 and are considered differentially abundant. Proteins showing no change in abundance are represented as blue dots. For clarity, only proteins of interest are shown.

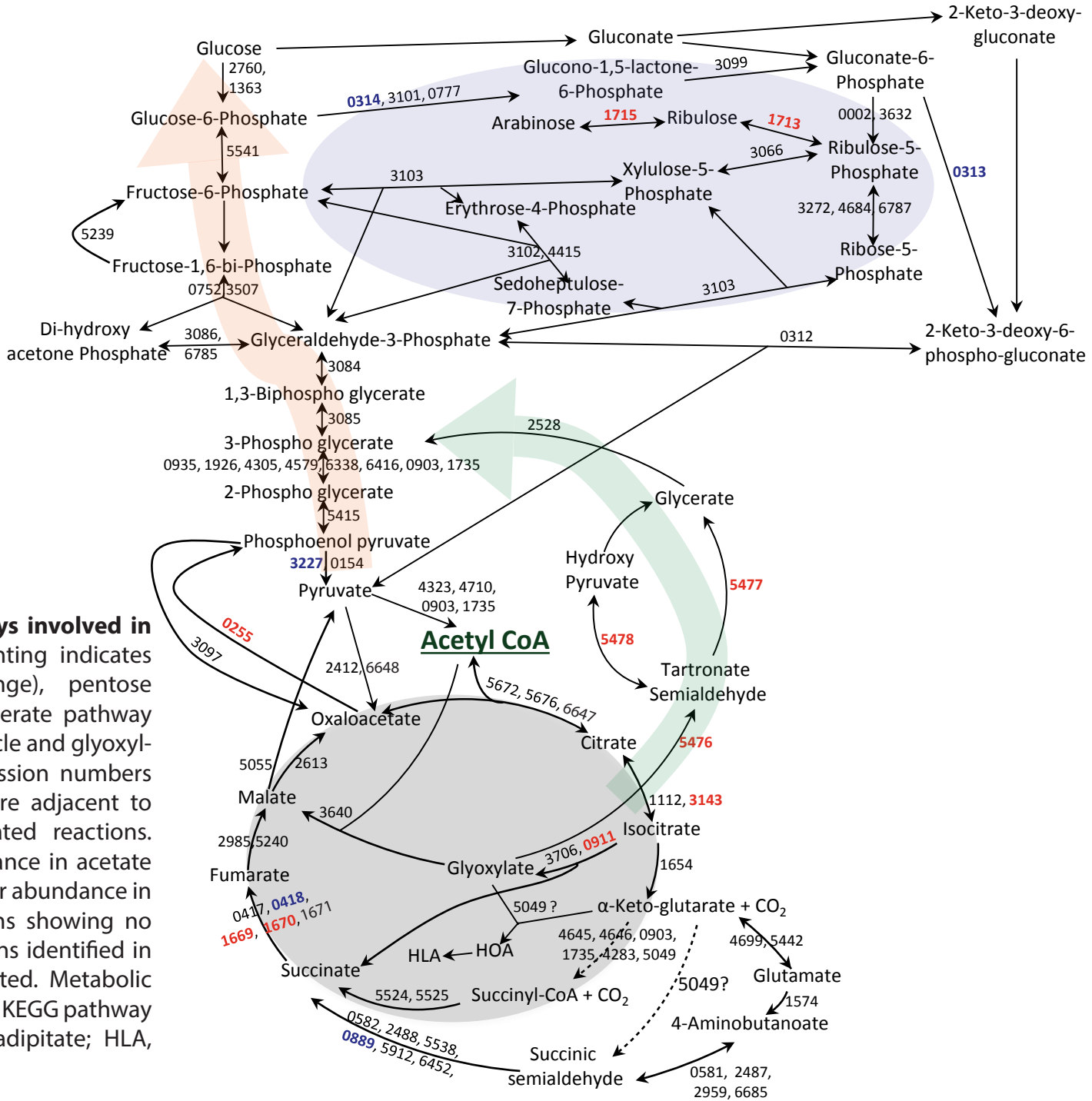

Supplemental Fig. S9. Pathways involved in acetate assimilation. Highlighting indicates gluconeogenic pathway (orange), pentose phosphate pathway (blue), glycerate pathway (green), and tricarboxylic acid cycle and glyoxylate shunt (grey). Enzyme accession numbers without the "MSMEG_" prefix are adjacent to arrows indicating their associated reactions. Proteins showing higher abundance in acetate are in red, proteins showing lower abundance in acetate are in blue, and proteins showing no change are in black. Only proteins identified in our proteomic analysis are indicated. Metabolic pathways are drawn according to KEGG pathway maps. HOA, 2-Hydroxy-3-oxo-adipitate; HLA, 5-Hydroxy levulinate.

Supplemental Fig. S10. Pathways involved in propionate assimilation. Highlighting indicates gluconeogenic pathway (orange), pentose phosphate pathway (blue), methylcitrate and methylmalonate pathways (pink), tricarboxylic acid cycle and glyoxylate shunt (grey). Enzyme accession numbers without the "MSMEG_" prefix are adjacent to arrows indicating their associated reactions. Proteins showing higher abundance in propionate are in red, proteins showing lower abundance in propionate are in blue, and proteins showing no change are in black. Only proteins identified in our proteomic analysis are indicated. Metabolic pathways are drawn according to KEGG pathway maps.